A00-31153

AIAA 2000-2047

Computation of flow noise using source terms in Linearized Euler's Equations

C. Bailly, C. Bogey and D. Juvé

Ecole Centrale de Lyon & UMR CNRS 5509
France

6th AIAA/CEAS
Aeroacoustics Conference
12-14 June 2000 / Lahaina, Hawaii

AIAA 2000-2047

Computation of flow noise using source terms in Linearized Euler's Equations*

Christophe Bailly† Christophe Bogey‡and Daniel Juvé§

Laboratoire de Mécanique des Fluides et d'Acoustique
Ecole Centrale de Lyon & UMR CNRS 5509
BP 163, 69131 Ecully cedex, France.

Abstract

An acoustic analogy combining Linearized Euler's Equations (LEE) as wave operator with suitable source terms is investigated to predict aerodynamic noise. The validity of this hybrid approach is evaluated by comparison with the acoustic far field provided directly by solving the Navier-Stokes equations. The method is applied to the case of two co-rotative vortices first in a medium at rest and second in a shear flow. Then, the noise generated by vortex pairings in a mixing layer is studied. A simplified formulation of LEE is proposed to prevent the exponential development of instability waves. The acoustic far field obtained by solving LEE is in good agreement with the solution given by direct calculation.

1. Introduction

Recent achievements of Computational AeroAcoustics (CAA) to predict aerodynamic noise are based on the direct calculation of the acoustic field by solving compressible Navier-Stokes equations. Freund[1] has thus carried on the work of the Stanford group with a Direct Numerical Simulation (DNS) of a Mach 0.9 jet with a Reynolds number $\mathrm{Re}_D = 3600$. Direct computation of the noise radiated by a subsonic 3-D jet remains however difficult, because of the large computing ressources required, and also because of numerical issues of CAA. In DNS, all turbulence scales, namely from the integral length scale to Kolmogorov's scale, are to be described. Colonius[2] has estimated the cost of a DNS of a subsonic turbulent flow providing both aerodynamic and acoustic fields. The total cost of an efficient numerical algorithm is proportional to $\mathrm{Re}_D^3/\mathrm{M}^4$, where M is the mean flow Mach number. In the same manner, the cost of a direct acoustic calculation using a Large Eddy Simulation (LES) is proportional to $\mathrm{Re}_D^2/\mathrm{M}^4$, assuming that the size of the resolved smallest eddies is given by the Taylor length scale. In that way, Bogey[3,4] *et al.* have performed a direct calculation of the noise radiated by a Mach 0.9 jet with a Reynolds number $\mathrm{Re}_D = 6.5 \times 10^4$.

Direct noise calculation for flows of practical interest, i.e. at high Reynolds number and usually at moderate Mach number, is quite expensive. In many engineering problems, only the time-dependent near aerodynamic field can be determined. An alternative to direct acoustic calculation consists in separating sound generation and sound propagation. Among the first hybrid methods, the most famous was proposed by Lighthill.[5] He derived a simple wave equation from the conservation laws of motion. The acoustic field is then obtained by solving a classical wave equation in which the source term is written as function of the aerodynamic field. A difficulty of Lighthill's analogy is to interpret the source term in which mean flow effects on the propagation are included.[6] Therefore, to account for all these effects, Lighthill's analogy requires a source volume containing all acoustic - flow interactions, and not only the turbulent region. With this aim in view, the velocity field used to built up source terms must be compressible.

A third-order wave operator was developped by Lilley[7] and Pridmore-Brown[8] to describe exactly acoustic propagation in unidirectional sheared mean

†Assistant Professor, Member AIAA

‡Postdoctoral student, Member AIAA

§Professor, Member AIAA

flows. The associated source term is mainly a non-linear function of the aerodynamic fluctuating velocity field. Many studies have been devoted to the resolution of Lilley's equation, analytically[9] or by using geometrical methods.[10] A time resolution can also be performed by transforming Lilley's equation into a system of first-order equations. By this way, Berman & Ramos[11] have calculated the radiation of a monopolar source in a jet mean flow provided by a $k-\epsilon$ closure. This idea was developed by Béchara[12] *et al.* with an approach based on Linearized Euler's Equations (LEE) accounting for refraction and convection effects in any sheared mean flows. In this approach, a source term is added into the right-hand side of LEE, and is built up from a synthesized turbulent field. The source term expression and the construction of a stochastic space-time turbulent field were improved later[13] and extended to 3-D geometries.[14,15]

The primary objective of this paper is to show that an acoustic analogy combining LEE with the source terms defined in Bailly[13] *et al.*, is able to predict aerodynamic noise. The validity of this hybrid approach is checked as follows. At first, a reference solution of the acoustic far-field is determined directly from Navier-Stokes equations. The aerodynamic field of this simulation is also used to built up the source terms introduced into LEE, and to estimate the mean flow. Finally, the acoustic field obtained by solving LEE is compared to the reference solution. LEE support acoustic disturbances as well as vortical and entropic disturbances. In particular, the acoustic mode and the vorticity mode are not decoupled when the mean flow is no longer uniform. As a result, physical growing instability waves are excited by the source terms. We propose to remove this coupling by considering a simplified formulation of LEE, without significant effects on noise propagation.

In section 2, we introduce the formulation of the source terms in 2-D LEE. Next three building block problems are considered. Sound field generated by two co-rotative vortices in a medium at rest is studied in section 3. In section 4, the same problem is investigated in the presence of a sheared mean flow with zero convection velocity. By this way, development of instability waves is neutralized. The noise generated by a mixing layer is then investigated in section 5. Influence of some quantities such as the mean value of source terms, and the removal of instability waves are also discussed. Definition of source terms in LEE, and connection with Lilley's equation is given in Appendix A. A validation of simplified LEE is shown in appendix B using the mean flow of the mixing layer.

2. Hybrid method based on LEE

2.1 Formulation

Consider small perturbations around a steady mean flow with density $\bar{\rho}$, velocity $\bar{\mathbf{u}} = (\bar{u}_1, \bar{u}_2)$ and pressure $\bar{p}$. These perturbations are governed by Linearized Euler's Equations:

$$\frac{\partial \mathbf{U}}{\partial t} + \frac{\partial \mathbf{E}}{\partial x_1} + \frac{\partial \mathbf{F}}{\partial x_2} + \mathbf{H} = \mathbf{S} \qquad (1)$$

where $\mathbf{U} = [\rho', \bar{\rho}u_1', \bar{\rho}u_2', p']^t$ is the unknown vector. The prime denotes the perturbation variable. Expressions of vectors $\mathbf{E}$, $\mathbf{F}$ and $\mathbf{H}$ are given in appendix A, and $\mathbf{S}$ represents a possible source term. The two notations $x_1 = x$ and $x_2 = y$ will be equivalent in this work.

In the present hybrid approach, generation is provided by source terms in the momentum equations of LEE written as[13]

$$\mathbf{S} = \left[0, S_1 = S_1^f - \overline{S_1^f}, S_2 = S_2^f - \overline{S_2^f}, 0\right]^t$$

where

$$S_1^f = -\frac{\partial \rho u_1' u_i'}{\partial x_i} \qquad S_2^f = -\frac{\partial \rho u_2' u_i'}{\partial x_i} \qquad (2)$$

The reasoning and assumptions behind this expression are explained in appendix A. The source term $\mathbf{S}^f$ is non-linear in velocity fluctuations, and its mean value is substracted. Density is provided by the aerodynamic calculation. The acoustic field is included in the source term, through density and fluctuating velocity, but this acoustic component is negligible compared to aerodynamic fluctuations.

For the three applications presented in sections 3 to 5, the Navier-Stokes equations are solved using the ALESIA code to obtain the acoustic far field. This reference solution will be compared to the result given by LEE forced with source terms (2). The near aerodynamic field is also used to build up these source terms, and to estimate the mean velocity field. LEE are then solved using the SPRINT code. The two solvers are briefly described in the next subsections.

2.2 Flow simulation: ALESIA

A 2-D and 3-D Large Eddy Simulation code - ALESIA for Appropriate Large Eddy SImulation for Aeroacoustics - has been developed.[3] Large Eddy Simulation (LES) is an alternative to Direct Numerical Simulation (DNS) for computing flows at higher Reynolds number. Only the larger structures are resolved, and the effects of the smaller scales are taken into account via the Smagorinsky subgrid scale model. Filtered Navier-Stokes equations are solved in a conservative form on a cartesian grid. The space derivatives are discretized with the DRP scheme of Tam & Webb,[16] and the time integration is performed by a fourth-order Runge-Kutta algorithm. Great care is taken in order to exploit directly the calculated acoustic field. The non-reflecting boundary conditions of Tam & Dong,[17] based on the asymptotic expression of Euler's equations in far field, are implemented. Outflow boundary conditions combined with a sponge zone are used to allow the exit of vortical structures. More details can be found in Bogey[3,18] *et al.* ALESIA can also be run without turbulence modelling to performe DNS.

2.3 Resolution of LEE: SPRINT

A 2-D and 3-D LEE solver - SPRINT for Sound PRopagation IN mean turbulent Turbulent flows - has been built using CAA techniques.[19] An outline of the numerical procedure is given below. LEE are solved using the DRP scheme of Tam & Webb[16] to evaluate spatial derivatives. The solution is advanced in time with a fourth-order Runge-Kutta integration. The radiation and outflow boundary conditions are based on an asymptotic formulation of LEE.[16] A sponge zone is needed when linear instability waves are convected by the sheared mean flow to dissipate aerodynamic fluctuations and to avoid reflections to be produced at the outflow boundary condition.

3. Sound field generated by two co-rotative vortices in a medium at rest

3.1 Flow simulation

In this first application, we consider the noise generated by two co-rotating vortices in a medium at rest. The initial tangential velocity distribution of each vortex is given by[20]

$$V_\theta(r) = -\frac{\Gamma r}{2\pi\left(r_c^2 + r^2\right)}$$

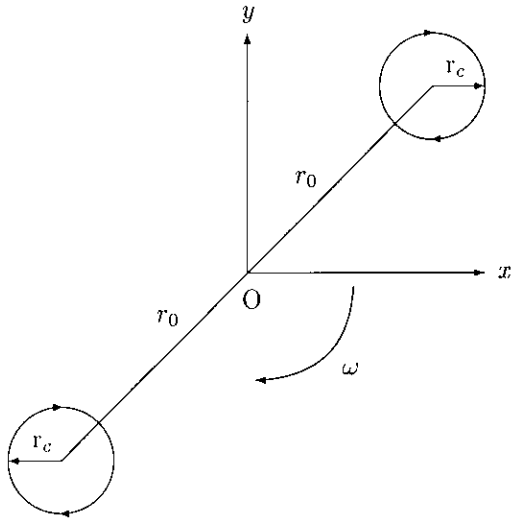

Figure 1: Sketch of the two co-rotative vortices.

where r is the radial distance from the vortex center, r_c is the core radius, and Γ is the circulation. The two vortices are separated by a distance $2r_0$, as illustrated in Figure 1. The angular frequency of the whole swirling flow is[21] $\omega = 2\pi f = \Gamma/(4\pi r_0^2)$, the period is $T = 8\pi^2 r_0^2/\Gamma$ and the co-rotating Mach number is $M_r = \Gamma/(4\pi r_0 c_0)$. In this study, the Mach number based on the maximum tangential velocity $V_{max} = \Gamma/(4\pi r_c)$ is $M = 0.5$, $r_c/r_0 = 2/9$, $M_r = 1/9$ and the Reynolds number is $\mathrm{Re} = \Gamma/\nu = 1.14 \times 10^5$.

The acoustic field is calculated directly by a Direct Numerical Simulation using the ALESIA code without turbulence modelling. The square computational mesh has 281×281 points with a regular step size $\Delta = r_0/18$ for the first thirty points in each direction from the center, and extends to $104r_0$. The time step is $\Delta t = 0.8\Delta/c_0$ which gives a rotating period $T \simeq 1272\Delta t$. The acoustic source associated with the two vortices is a rotating quadrupole,[21] and the acoustic frequency is $f_a = 2 \times f$ because of the source symmetry. The mesh is stretched so that at least 7 points are in the acoustic wavelength $\lambda_a = 28.3r_0$. The simulation runs for 12×10^3 iterations.

After a transient period, an acoustic radiation at the frequency f_a is observed during about six periods T of rotation. Then, the two vortices begin to merge with an increase of the amplitude and frequency of the acoustic signal. A peak in amplitude is reached

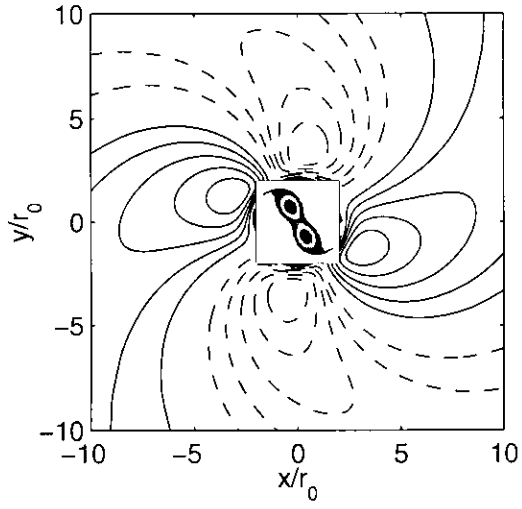

Figure 2: Snapshot of the near field vorticity surrounded by 7 iso-contours of the dilatation field defined from 8 s^{-1} to 56 s^{-1} with constant increment. ——— positive values, − − − negative values.

when the two vortices coalesce and the amplitude diminishes significantly after merger. The description of the vortex pairing is not shown in this paper.[3] A snapshot of the near field dilatation $\Theta = \nabla.\mathbf{u}$ is displayed in Figure 2. The dilatation is directly connected to the acoustic pressure time derivative in a medium at rest by $\Theta = -(1/\rho_0 c_0^2)\partial p/\partial t$. The use of the dilatation as acoustic variable allows to get rid of the low-frequency small drift of the mean pressure field.[22] There is actually no pressure drift in this first application but we will use anyway dilatation to represent acoustic fields. The typical double-spiral pattern of a rotating quadrupolar source is obtained as shown analytically by Powell,[21] and numerically by Lee[20] *et al.* and Mitchell[23] *et al.*

3.2 Application of LEE

Aerodynamic fluctuations provided by the DNS are now used to build up the source terms (2). They are recorded every Δt, from $t = 2000\Delta t$ to $6000\Delta t$, on a square domain of size $9.5r_0$ corresponding to a 121×121 grid. The source domain is large enough to avoid significant truncation of the source terms. Their amplitudes on the boundaries are less than 1% of their maximum amplitude reached in the domain. Linearized Euler's Equations (1) are then solved on the same mesh than the previous DNS, and with the same time step since the numerical algorithms are identical.

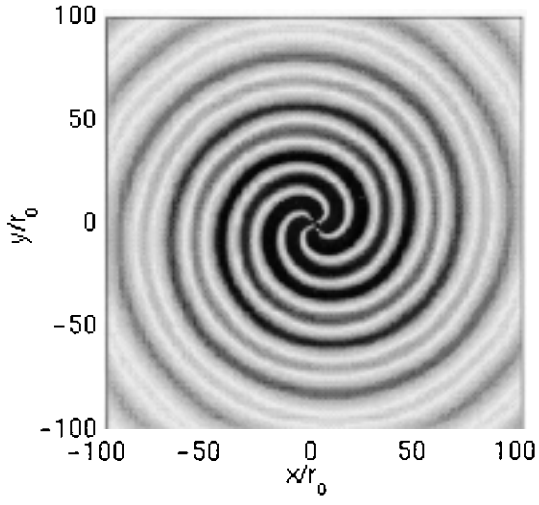

Figure 3: Representation of the dilatation field computed by solving LEE with source term (2) at time $t = 6000\Delta t$. Levels are given from -15 to 15 s^{-1}.

The dilatation field predicted by LEE is presented in Figure 3, and is in good agreement with the reference solution.[3] To provide a more quantitative comparison, dilatation profiles obtained by solving LEE and from the DNS are compared in Figure 4. The same result would be obtained by applying Lighthill's analogy since there is no mean flow. This simple example shows that the acoustic analogy based on LEE with the source term (2) is able to provide correctly the radiated acoustic field.

4. Sound field generated by two co-rotative vortices in a sheared mean flow

4.1 Flow simulation

We still consider the case of two co-rotatives vortices represented in Figure 1, but they are now placed in a sheared flow with a zero convection velocity, as illustrated in Figure 5. The following hyperbolic tangent profile is chosen:

$$u_1(y) = \Delta U \tanh(2y/\delta_\omega) \qquad (3)$$

with $\Delta U = 0.125c_0$. The vorticity thickness is taken as $\delta_\omega = 4r_0$, where r_0 is half the distance between the two vortices. Mean density and mean pressure are constant. The acoustic reference solution is again calculated directly by DNS. The middle part of the DNS mesh of section 3.1 is used to obtain a cartesian grid of 251×251 points which extends to $55r_0$ in each direction.

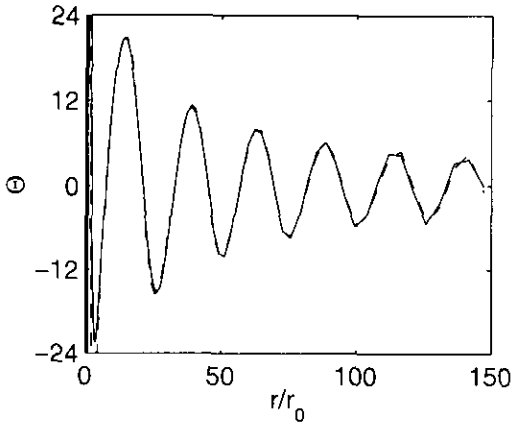

Figure 4: Dilatation profiles obtained along line $x = y$ with $x > 0$ and at time $t = 6000\Delta t$, by solving LEE with source term (2) $- - -$ and from the DNS ——— . Levels are given in s^{-1}.

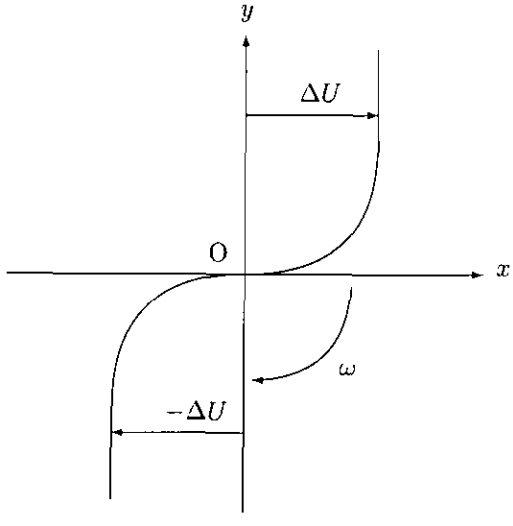

Figure 5: Sketch of the sheared flow with a zero convection velocity. The two flow velocities are $\pm\Delta U = \pm 0.125 c_0$ and the vorticity thickness is $\delta_\omega = 4r_0$.

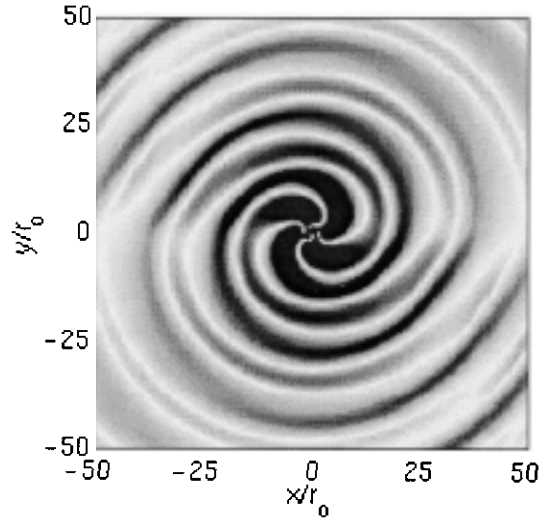

Figure 6: Dilatation field at time $t = 2500\Delta t$, radiated by co-rotatives vortices placed in a sheared mean flow with a zero convection velocity. DNS result. Levels of dilatation from -50 to 50 s^{-1}.

After a numerical transient, the merging process can be described in the three usual steps. The two vortices begin to roll around each other, then the two cores coalesce with production of vorticity filaments, and a final circular vortex is formed. In our configuration, however, the rotation of the mean flow is added to the rotation induced by the two spinning vortices. Thus, the period of rotation is smaller, $T \simeq 750\Delta t$, corresponding to an acoustic wavelength of $\lambda_a \simeq 16.7 r_0$. Moreover, there are only three periods of rotation before merger. The dilatation field obtained by DNS at time $t = 2500\Delta t$ is shown in Figure 6. The dilatation variable is related to the acoustic pressure by:

$$\Theta = -\frac{1}{\rho_0 c_0^2}\left(\frac{\partial p}{\partial t} \pm \Delta U \frac{\partial p}{\partial x}\right)$$

for the upper stream and lower stream respectively. In comparison with Figure 4, wave fronts are ovalized due to mean flow convection effects. There are also refraction effects, but they are not important since the shear-layer vorticity thickness $4r_0$ is small with respect to the acoustic wavelength λ_a.

4.2 Application of LEE

Source terms are recorded every Δt between $t = 200\Delta t$ and $t = 2500\Delta t$ on the same square domain as in section 3.2. LEE are solved by using the analytic mean velocity profile (3). The transverse mean

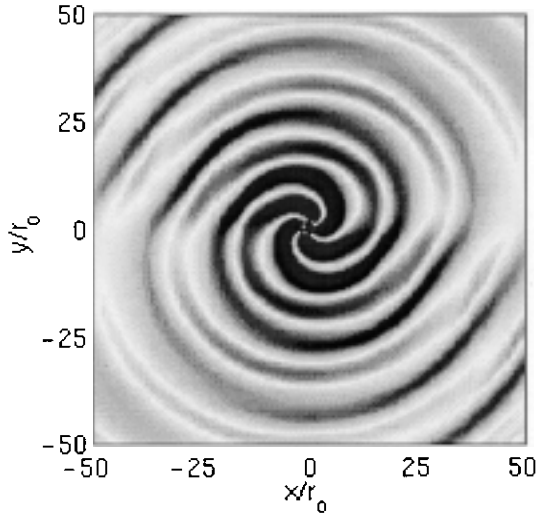

Figure 7: Dilatation field at time $t = 2500\Delta t$, radiated by co-rotatives vortices placed in a sheared flow with a zero convection velocity. LEE result. Levels of dilatation are given from -50 to 50 s^{-1}.

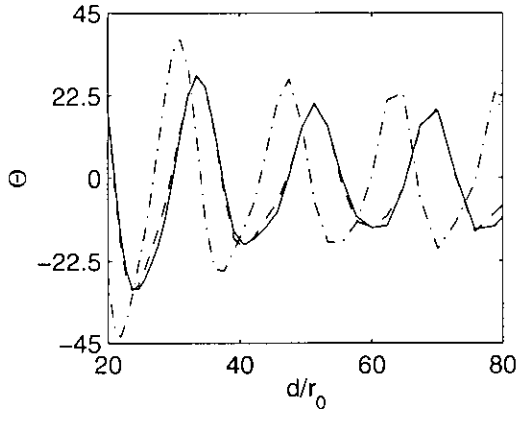

Figure 8: Dilatation profiles obtained by solving LEE with source term (2) $- - -$, by solving LEE without mean flow $- \cdot - \cdot$, and from the DNS ——— . Profiles are taken along line $x = y$ with $x > 0$ and at time $t = 2500\Delta t$, $d = \sqrt{x^2 + y^2}$ and levels are given in s^{-1}.

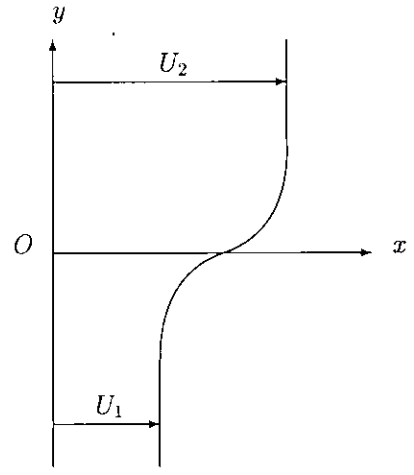

Figure 9: Sketch of the mixing layer.

velocity is zero while mean pressure and density are taken to be constant, with the same values used to initialize the DNS. Figure 7 shows the dilatation field predicted by LEE. This result is consistent with the DNS field displayed in Figure 6. No instability wave is observed since the shear flow has no convection velocity.

Dilatation profile along a diagonal line of the computational domain is plotted in Figure 8. It is in very good agreement with the DNS profile. Importance of mean flow effets can be underlined by solving LEE without mean velocity field, by setting $u_0 \equiv 0$. This point is clearly illustrated with the corresponding dilatation profile shown in Figure 8.

5. Sound field generated by a mixing layer

5.1 Flow simulation

In this last application, the noise generated by a subsonic mixing layer between two flows at $U_1 = 40$ and $U_2 = 160$ m.s^{-1} is investigated. The inflow hyperbolic tangente profile is given by:

$$u_1(y) = \frac{U_1 + U_2}{2} + \frac{U_2 - U_1}{2} \tanh\left(\frac{2y}{\delta_\omega(0)}\right) \quad (4)$$

where $\delta_\omega(0)$ is the initial vorticity thickness. One also defines the convection velocity as $U_c = (U_1 + U_2)/2 = 100$ m.s^{-1} and the Reynolds number $\mathrm{Re} = U_c\delta_{\omega(0)}/\nu = 12800$. The flow is forced at its fundamental frequency f_0 and its first subharmonic $f_0/2$ in order to fix the location of vortex pairings around $x \simeq 70\delta_\omega(0)$ in the mixing layer. The acoustic field is calculated directly by a Large Eddy Simulation

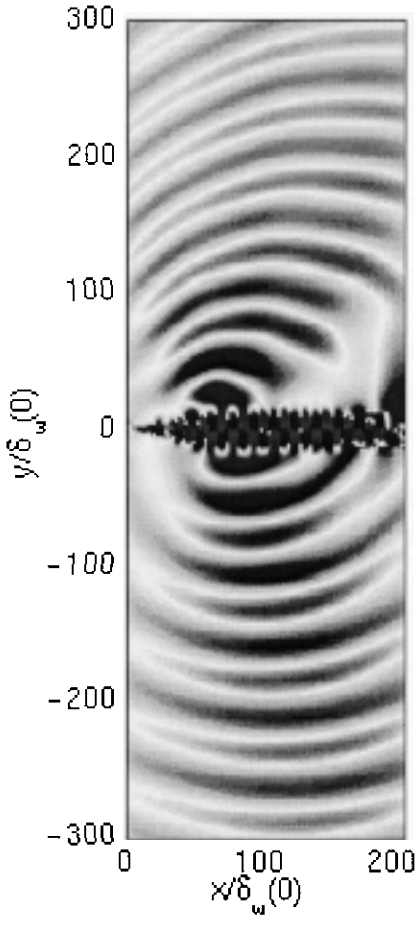

Figure 10: Dilatation field obtained by LES on the whole physical computational domain. Levels are given from -1.6 to 1.6 s^{-1}.

using the ALESIA code. All the details of the simulation as well as acoustic results and comparisons with Lighthill's analogy can be found in Bogey[3,18] *et al.* The dilatation field is displayed in Figure 10 on the whole physical computational domain. Wave fronts are observed coming from the location of pairings with an acoustic wavelength $\lambda_{f_p} = 51.5\delta_\omega(0)$, corresponding to the frequency of pairings $f_p = f_0/2$. Convection effects are visible and are well marked in the downstream direction for the upper flow.

5.2 Application of LEE

The source volume extends from $5\delta_\omega(0)$ to 235 $\delta_\omega(0)$ in the axial direction, and from $-50\delta_\omega(0)$ to $50\delta_\omega(0)$ in the transversal direction. The mesh used in the source region is coarser since only every two points of the LES grid in the two coordinate directions is kept. Source terms are recorded every two

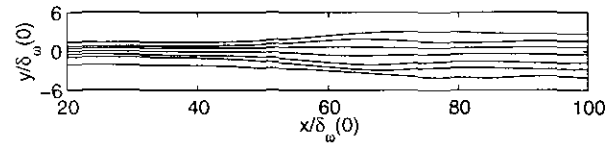

Figure 11: Mean axial velocity contours in the near field region provided by the LES. Contour levels: 44, 52, 68 ,100, 132, 148, 156 $m.s^{-1}$.

time steps during the last 5400 iterations of the LES, corresponding to 16 pairing periods. By this way, $\Delta t_{LEE} = 2\Delta t_{LES}$ and, space or time interpolations of source terms are avoided. The mean velocity field is provided by the LES whereas mean density and pressure are constant. Figure 11 displays the mean axial velocity contours in the shear flow region, and shows clearly the location of vortex pairings around $x \simeq 70\delta_\omega(0)$ with a doubling of the shear-layer thickness.

Growing instability waves can be excited by source terms in LEE through the mean shear $\partial\bar{u}_1/\partial x_2$ in the vector $\mathbf{H}$, see appendix A. In order to prevent the development of linear instability waves, we set $\mathbf{H} \equiv 0$. The reader is referred to appendix B for a discussion of this assumption. A test case is also performed to show acoustic propagation is not modified significantly. This simplified formulation of LEE allows to consider only the acoustic mode. Three particular points are now investigated.

Contribution of the average of source terms

The source term (2) can be decomposed as $\mathbf{S} = \mathbf{S}^f - \overline{\mathbf{S}^f}$. Figure 12 represents the contribution of the average $\overline{\mathbf{S}^f}$ of the source terms $\mathbf{S}^f$ in the pressure field. To solve LEE, the mean velocity field is taken as zero in this paragraph. Figure 13 shows the radial pressure profiles associated with the three source terms $\mathbf{S}$, $\mathbf{S}^f$ and $\overline{\mathbf{S}^f}$. To understand these curves, we consider the following basic problem of an incompressible aerodynamic field. The incompressible pressure induced by a solenoïdal velocity field $\mathbf{u}_s$ is defined by the relation:

$$p^s(\mathbf{x}) = \frac{1}{4\pi}\int_V \frac{\partial^2 \rho u_i^s u_j^s}{\partial y_i \partial y_j}(\mathbf{y})\,\frac{d\mathbf{y}}{|\mathbf{x}-\mathbf{y}|}$$

in 3-D, and:

$$p^s = \frac{1}{4\pi}\frac{\partial^2}{\partial x_i \partial x_j}\left(\frac{1}{x}\right)\int_V \rho u_i^s u_j^s d\mathbf{y} \sim \mathcal{O}\left(\frac{1}{x^3}\right)$$

as $x \to \infty$. The pressure p^s decreases faster than

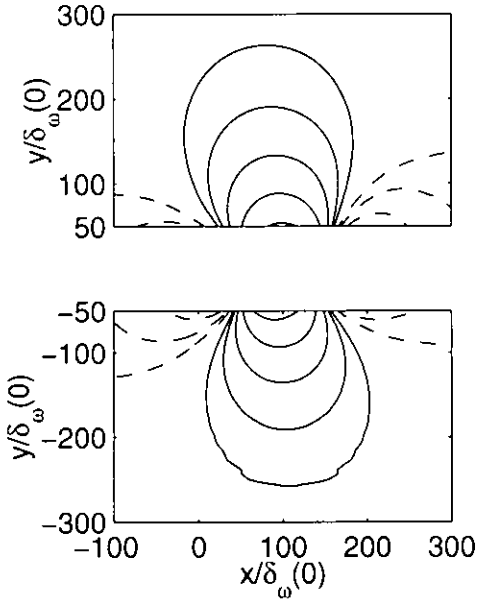

Figure 12: Contribution of the average $\bar{\mathbf{S}}^f$ in the pressure field $p - p_0$, calculated by LEE. ——— , 5 positive iso-contours of pressure from 0.5 to 8 Pa, – – – , negative iso-contours. The mean velocity field is taken as zero.

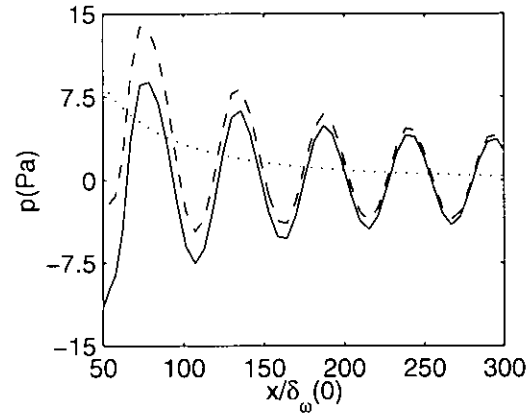

Figure 13: Pressure profile at $x = 90\delta_\omega(0)$ by solving LEE: ——— source term $\mathbf{S}$, – – – source term $\mathbf{S}^f$, ····· contribution of the source term $\overline{\mathbf{S}^f}$.

acoustic waves, and we have a similar result in 2-D with $p^s \sim 1/x^2$. Thus, to get the correct radiated acoustic pressure in the near field region, it is recommended to substract the time-average of source terms in LEE.

Inappropriate formulation of the source term

The source term introduced in LEE must be determined from the fluctuating velocity field, and not from the instantaneous velocity field provided by LES. In this last case, the source term

$$\begin{aligned} S_i^t &= \frac{\partial \rho u_i u_j}{\partial x_j} - \overline{\frac{\partial \rho u_i u_j}{\partial x_j}} \\ &= \frac{\partial \rho \bar{u}_i u_j'}{\partial x_j} + \frac{\partial \rho u_i' \bar{u}_j}{\partial x_j} + \underbrace{\frac{\partial \rho u_i' u_j'}{\partial x_j} - \overline{\frac{\partial \rho u_i' u_j'}{\partial x_j}}}_{S_i^f} \end{aligned}$$

contains a linear contribution in velocity fluctuations. The acoustic analogy based on LEE is developed precisely to eliminate the ambiguous interpretation of this kind of terms. Figure 14 shows the pressure field provided by LEE using the source term $\mathbf{S}^t$. Mean flow effects, and more specially refraction effects are clearly overestimated, as shown

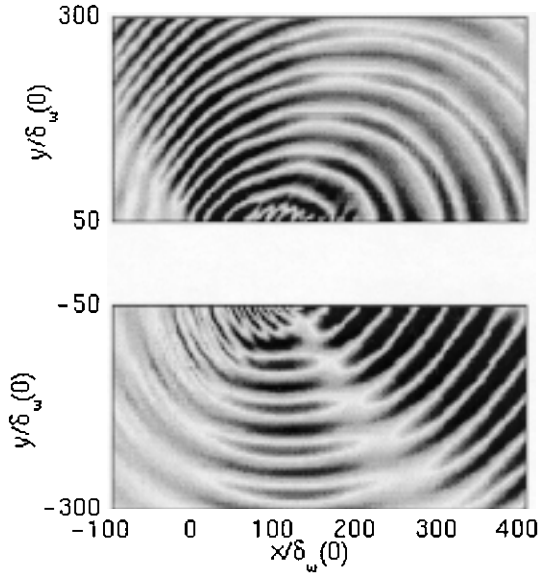

Figure 14: Dilatation field obtained by solving LEE with an inappropriate formulation of the source terms, $\mathbf{S} = \mathbf{S}^t$. Levels are given from -1.6 to 1.6 s^{-1}.

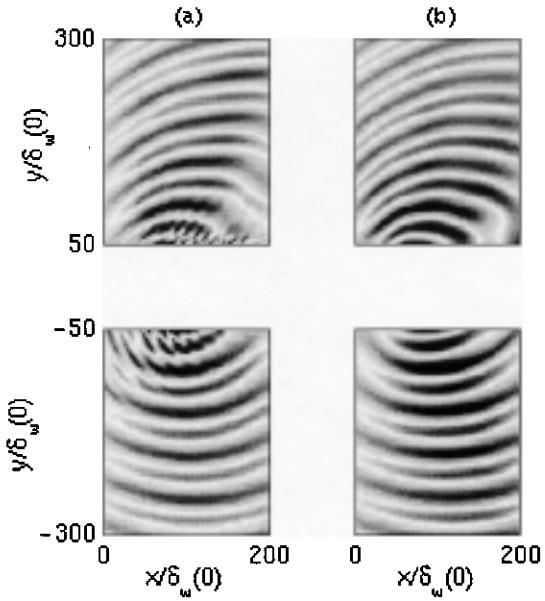

Figure 15: Representation of the dilatation field, (a) from LEE with the source term (2), (b) from LES. Levels are given from -1.6 to 1.6 s^{-1}.

by comparison with the DNS result of Figure 10.

Simplified formulation of LEE

LEE are now solved with the source term given by expression (2), and the calculated dilatation field is compared with the LES result in Figure 15. Recall that the mean velocity field provided by the LES is used to linearize Euler's equations, and that the term **H** is cancelled. The two acoustic fields are consistent, and this point is made clear in Figure 16 by comparison with corresponding dilatation profiles. The two profiles are in excellent agreement in amplitude and in phase, except in the source region where the acoustic field is greatly dominated by the aerodynamic field. The importance of mean flow effects is shown in Figure 17. LEE are solved using the source term (2), without mean velocity field in the case (a), and with the mean velocity field in the case (b). Mean flow effects strongly affect the radiated field.

6. Concluding remarks

In this study, we show that an acoustic analogy based on Linearized Euler's Equations is able to provide aerodynamic noise, accounting for the major part of mean flow effects. The expression of term sources is validated without using ad hoc assumptions since the aerodynamic velocity field as well

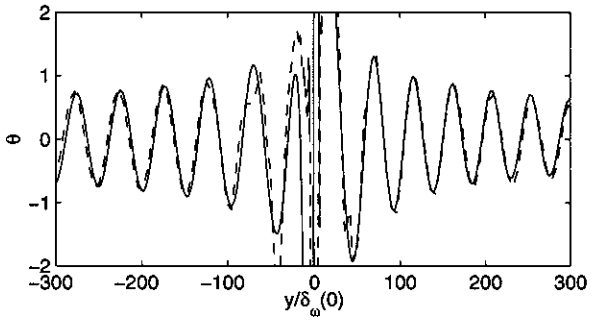

Figure 16: Radial dilatation profiles at the pairing location $x = 70\delta_\omega(0)$. − − − from LEE with source term (2), ——— from LES, reference solution.

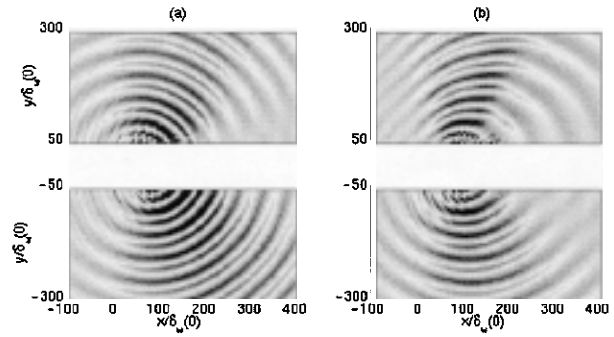

Figure 17: Representation of the dilatation field from LEE: (a) without taking account for mean flow effects by setting $\bar{u}_1 = \bar{u}_2 \equiv 0$, (b) with the mean flow effects. Levels are given from -1.6 to 1.6 s^{-1}.

as the reference acoustic far field are given directly by solving the compressible Navier-Stokes equations. Growing instability waves are removed by considering a simplified formulation of LEE, in which the mean shear term corresponding to the second derivative of the velocity profile in Rayleigh's stability equation is cancelled. Further studies are needed in the case of high-frequency radiation to evaluate the part of refraction effects taken into account by the simplified wave operator, and to analyse the associated stability equation. These results support also previous works developed by one of the authors.[13]

Appendix A: Wave equation from LEE

The three vectors **E**, **F** and **H** of Linearized Euler's Equations (1) are given respectively by:

$$\mathbf{E} = \begin{pmatrix} \rho' \bar{u}_1 + \bar{\rho} u_1' \\ \bar{u}_1 \bar{\rho} u_1' + p' \\ \bar{u}_1 \bar{\rho} u_2' \\ \bar{u}_1 p' + \gamma \bar{p} u_1' \end{pmatrix} \quad \mathbf{F} = \begin{pmatrix} \rho' \bar{u}_2 + \bar{\rho} u_2' \\ \bar{u}_2 \bar{\rho} u_1' \\ \bar{u}_2 \bar{\rho} u_2' + p' \\ \bar{u}_2 p' + \gamma \bar{p} u_2' \end{pmatrix}$$

and

$$\mathbf{H} = \begin{pmatrix} 0 \\ (\bar{\rho} u_1' + \rho' \bar{u}_1) \dfrac{\partial \bar{u}_1}{\partial x_1} + (\bar{\rho} u_2' + \rho' \bar{u}_2) \boxed{\dfrac{\partial \bar{u}_1}{\partial x_2}} \\ (\bar{\rho} u_1' + \rho' \bar{u}_1) \dfrac{\partial \bar{u}_2}{\partial x_1} + (\bar{\rho} u_2' + \rho' \bar{u}_2) \dfrac{\partial \bar{u}_2}{\partial x_2} \\ (\gamma - 1) p' \nabla . \bar{\mathbf{u}} - (\gamma - 1) \mathbf{u}' . \nabla \bar{p} \end{pmatrix}$$

The term **H** is zero for an uniform mean flow field. A part of the refraction effects can be attributed to **H**.

In order to derive a wave equation on the pressure fluctuation p' including all acoustic - mean flow interactions, LEE must be combined to eliminate all the terms involving velocity fluctuations. By this way, the simplest nontrivial differential equation for the pressure is obtained in the case of a strictly parallel mean flow, i.e. $\bar{u}_1 = \bar{u}_1(x_2)$ and $\bar{u}_2 = 0$. Since the steady mean flow satisfies Euler's equations, the mean pressure is necessarily constant with $\bar{p} = p_0$, whereas the mean density and speed of sound are only function of the transverse coordinate x_2, $\bar{\rho} = \bar{\rho}(x_2)$ and $\bar{c} = \bar{c}(x_2)$. Moreover entropy fluctuations are simply convected by the mean flow without production, and if we assume $s' \equiv 0$ at a given time, then $p' = \bar{c}^2 \rho'$. Applying the convective derivative based on the mean flow velocity $\bar{D}/\bar{D}t = \partial/\partial t + \bar{u}_1 \partial/\partial x_1$ to the continuity equation, taking the divergence of the momentum equation, and substracting the two expressions lead to Phillips' wave equation:

$$\frac{\bar{D}^2 \rho'}{\bar{D}t^2} - \nabla^2 p' - 2\bar{\rho} \frac{\partial u_2'}{\partial x_1} \frac{d\bar{u}_1}{dx_2} = -\nabla . \mathbf{S}$$

To eliminate the linear term in u_2', the operator $\bar{D}/\bar{D}t$ is applied again to the transverse momentum equation. Thus, one finds:

$$\frac{\bar{D}}{\bar{D}t} \left[\frac{1}{\bar{c}^2} \frac{\bar{D}^2 p'}{\bar{D}t^2} - \nabla^2 p' \right] + 2 \frac{d\bar{u}_1}{dx_2} \frac{\partial^2 p'}{\partial x_1 \partial x_2} = \Lambda \qquad (5)$$

where the source term is:

$$\Lambda = -\frac{\bar{D}}{\bar{D}t} \nabla . \mathbf{S} + 2 \frac{d\bar{u}_1}{dx_2} \frac{\partial S_2}{\partial x_1}$$

Equation (5) derived from LEE, corresponds exactly to the simplified formulation of Lilley's equation[7] obtained for a unidirectional sheared mean flow. An unambiguous interpretation of Lilley's wave equation can be provided only in this case.[24] Then the source term **S** must be written as

$$\Lambda = \frac{\bar{D}}{\bar{D}t} \frac{\partial^2 \rho u_i' u_j'}{\partial x_i \partial x_j} - 2 \frac{d\bar{u}_1}{dx_2} \frac{\partial^2 \rho u_2' u_j'}{\partial x_1 \partial x_j} \qquad (6)$$

by choosing $S_i = -\partial \rho u_i' u_j' / \partial x_j$ to closely follow Lilley's equation. The source term Λ contains two parts. The first one corresponds to the convection by the mean flow of $\nabla . \mathbf{S}$ when the second one is connected to the mean velocity shear. But the "self-noise" term and the "shear-noise" term in Lilley's equation are quadratic in velocity fluctuations, which is not the case in Lighthill's analogy.

Appendix B: Simplified wave operator based on LEE

Source terms in LEE excite growing instability waves in sheared flows. Instability waves are indeed governed by the homogeneous linearized Euler equations (1). For a strictly parallel mean flow $\bar{u}_1 = \bar{u}_1(x_2)$, and assuming incompressible perturbations to keep the problem as simple as possible, Rayleigh's stability equation is given by:

$$\left(\bar{u}_1 - \frac{\omega}{k} \right) \left[\frac{d^2 \hat{u}_2}{dx_2^2} - k^2 \hat{u}_2 \right] - \frac{d^2 \bar{u}_1}{dx_2^2} \hat{u}_2 = 0 \qquad (7)$$

where the transverse velocity u_2' corresponds to the real part of $\hat{u}_2(x_2) \exp[i(kx - \omega t)]$. The incompressibility assumption allows to write the same equation for the stream function ψ since $\hat{u}_2 = -ik\phi$ where $\psi = \phi(x_2) \exp[i(kx - \omega t)]$. For spatial instability analysis, the axial wavenumber $k = k_r + ik_i$ is complex whereas the angular frequency ω is real. Thus, perturbations are unstable when the imaginary part of the wavenumber is negative, i.e. $k_i < 0$.

The simplified wave operator used in section 5 is obtained by cancelling the vector **H**, which writes as $[0, \bar{\rho} u_2' d\bar{u}_1/dx_1, 0, 0]^t$ for a strictly parallel mean flow. The new stability equation corresponding to this simplified operator can be written as:

$$\left(\bar{u}_1 - \frac{\omega}{k} \right) \left[\frac{d^2 \hat{u}_2}{dx_2^2} - k^2 \hat{u}_2 \right] + \frac{d\bar{u}_1}{dx_2} \frac{d\hat{u}_2}{dx_2} = 0 \qquad (8)$$

and the homogeneous wave equation associated with equation (5) is:

$$\frac{\bar{D}}{\bar{D}t} \left[\frac{1}{\bar{c}^2} \frac{\bar{D}^2 p'}{\bar{D}t^2} - \nabla^2 p' \right] + \frac{d\bar{u}_1}{dx_2} \frac{\partial^2 p'}{\partial x_1 \partial x_2} = \Lambda \qquad (9)$$

Note that the second derivative of the mean velocity $\bar{u}_2$ which plays a crucial role in Rayleigh's equation (7) with the inflexion point theorem, does not appear in (8). The consequence for acoustic propagation is that the refraction term proportional to $d\bar{u}_1/dx_2$ differs from a factor 2 with respect to Lilley's equation (5).

Consider now the response of LEE to time-harmonic forcing of the mixing layer mean flow studied in section 5. The mean axial velocity is expressed as:

$$\bar{u}_1(x,y) = \frac{U_1+U_2}{2} + \frac{U_2-U_1}{2}\tanh\left(\frac{2y}{\delta_\omega}\right) \quad (10)$$

where the vorticity thickness is taken as:

$$\delta_\omega(x) = \delta_\omega(0)\left[\frac{3}{2} + \frac{1}{2}\tanh\left(\frac{x-70}{10}\right)\right]$$

to fit the LES result shown in Figure 11. The vector $\mathbf{S}$ represents a monopolar source:

$$\mathbf{S} = \epsilon \sin(\omega t)\, e^{-\alpha\left(x_1^2+x_2^2\right)}\, \left[1/c_0^2, 0, 0, 1\right]^t$$

with the same angular frequency $\omega = 2\pi f_p$ as the vortex pairing frequency, and located at $x = 70\delta_\omega(0)$. The amplitude of the source is $\epsilon = 10^{-4}$. The value of the coefficient α is $\ln 2/b^2$ with a half-width of $b = 3 \times \Delta$, a step size of $\Delta = 0.24\delta_\omega(0)$ in the shear region and a mesh of 651×501 points. The pressure field obtained by solving LEE with $\mathbf{H} = 0$ is represented in Figure 18(a), and the difference with the pressure field given by a full resolution of LEE is plotted in Figure 18(b). As expected, instability waves are created and convected in the downstream direction. However the resulting error for the acoustic field is small, since refraction effects are limited in our case where the acoustic wavelength $\lambda = 51.5\delta_\omega(0)$ is much larger than the shear layer thickness. Radial pressure profiles are compared in Figure 19, and confirm more quantitatively this result.

Acknowledgments

Computing time was supplied by Institut du Développement et des Ressources en Informatique Scientifique (IDRIS - CNRS). The authors gratefully acknowledge Philippe Lafon from EDF for stimulating discussions and for financial support.

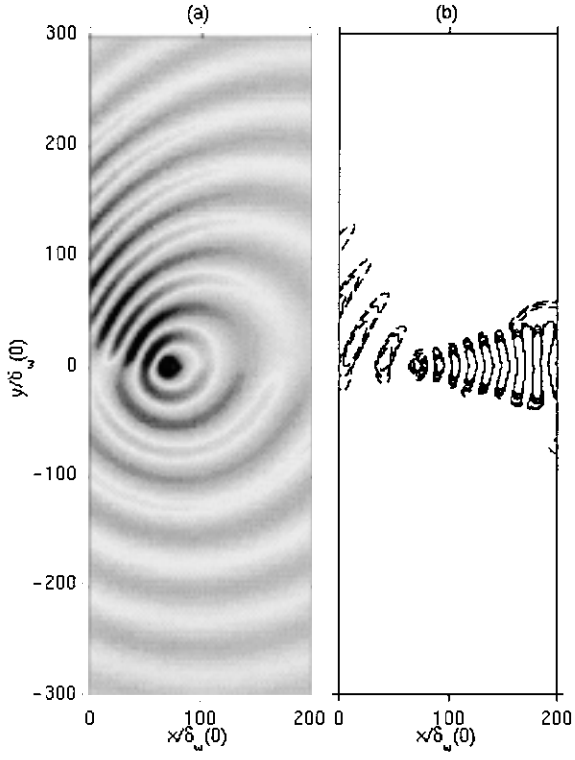

Figure 18: (a) Pressure field from LEE with $\mathbf{H} = 0$, levels from -5×10^{-6} to 5×10^{-6}. (b) Difference between pressure fields from LEE with $\mathbf{H} = 0$ and from full LEE. Contour levels: $- - -$ $[1.\,;2.\,;4.] \times 10^{-7}$, ——— $[1.6\,;3.2\,;6.4] \times 10^{-6}$.

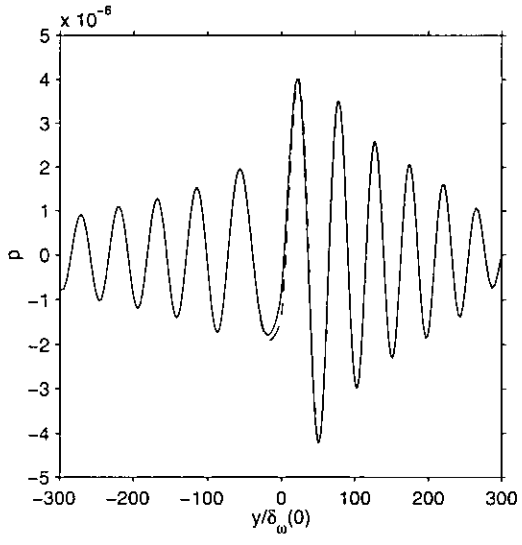

Figure 19: Radial pressure profiles at $x = 25\delta_\omega(0)$: ——— pressure profile from LEE with $\mathbf{H} = 0$, $- - -$ pressure profile from full LEE.

References

[1]FREUND, J.B., 1999, Acoustic sources in a turbulent jet: a direct numerical simulation study, AIAA Paper 99-1858.

[2]COLONIUS, T., 1997, Lectures on Computational Aeroacoustics, *von Karman Institute for Fluid Dynamics*, Lectures Series 1997-07.

[3]BOGEY, C., 2000, Calcul direct du bruit aérodynamique et validation de modèles acoustiques hybrides, Ph. D. thesis of Ecole Centrale de Lyon, No. 2000-11.

[4]BOGEY, C., BAILLY, C. & JUVÉ, D., 2000, Computation of the sound radiated by a 3-D jet using Large Eddy Simulation, AIAA Paper 2000-2009.

[5]LIGHTHILL, M.J., 1952, On sound generated aerodynamically - I. General theory, *Proc. Roy. Soc. London*, **211**, A 1107, 564-587.

[6]RIBNER, H.S., 1996, Effects of jet flow on jet noise via an extension to the Lighthill model, *J. Fluid Mech.*, **321**, 1-24.

[7]LILLEY, G.M., 1972, The generation and radiation of supersonic jet noise. Vol. IV - Theory of turbulence generated jet noise, noise radiation from upstream sources, and combustion noise. Part II: Generation of sound in a mixing region, *U.S. Air Force Aero-Propulsion Lab.*, AFAPL-TR-72-53, Vol. 4.

[8]PRIDMORE-BROWN, D.C., 1958, Sound propagation in a fluid flowing through an attenuating duct, *J. Fluid Mech.*, **4**, 393-406.

[9]GOLDSTEIN, M.E., 1981, Aeroacoustics of turbulent shear flows, *Annu. Rev. Fluid Mech.*, **16**, 263-285.

[10]CANDEL, S.M., 1977, Numerical solution of conservation equations arising in linear wave theory: application to aeroacoustics, *J. Fluid Mech.*, **83**(3), 465-493.

[11]BERMAN, C. & RAMOS, J., 1989, Simultaneous computation of jet turbulence and noise, AIAA Paper 89-1091.

[12]BÉCHARA, W., BAILLY, C., LAFON, P. & CANDEL, S., 1994, Stochastic approach to noise modeling for free turbulent flows, *AIAA Journal*, **32**(3), 455-463.

[13]BAILLY, C., LAFON, P. & CANDEL, S., 1995, A stochastic approach to compute noise generation and radiation of free turbulent flows, AIAA Paper 95-092.

[14]LONGATTE, E., LAFON, P. & CANDEL, S., 1998, Computation of noise generation in internal flows, AIAA Paper 98-2332.

[15]BAILLY, C. & JUVÉ, D., 1999, A stochastic approach to compute subsonic noise using linearized Euler's equations, AIAA Paper 99-1872.

[16]TAM, C.K.W. & WEBB, J.C., 1993, Dispersion-relation-preserving finite difference schemes for computational acoustics, *J. Comput. Phys.*, **107**, 262-281.

[17]TAM, C.K.W. & DONG, Z., 1996, Radiation and outflow boundary conditions for direct computation of acoustic and flow disturbances in a nonuniform mean flow, *J. Comput. Acous.*, **4**(2), 175-201.

[18]BOGEY, C., BAILLY, C. & JUVÉ, D., 1999, Computation of mixing layer noise using Large Eddy Simulation, AIAA Paper 99-1871, accepted in the AIAA Journal.

[19]BAILLY, C. & JUVÉ, D., 2000, Numerical solution of acoustic propagation problems using linearized Euler's equations, *AIAA Journal*, **38**(1), 22-29.

[20]LEE, D.J. & KOO, S.O., 1995, Numerical study of sound generation due to a spinning vortex pair, *AIAA Journal*, **33**(1), 20-26.

[21]POWELL, A., 1964, Theory of vortex sound, *J. Acoust. Soc. Am.*, **36**(1), 177-195.

[22]COLONIUS, T., LELE, S.K. & MOIN, P., 1997, Sound generation in a mixing layer, *J. Fluid Mech.*, **330**, 375-409.

[23]MITCHELL, B.E., LELE, S.K. & MOIN, P., 1995, Direct computation of the sound from a compressible co-rotating vortex pair, *J. Fluid Mech.*, **285**, 181-202.

[24]GOLDSTEIN, M.E., 1976, Aeroacoustics, *McGraw-Hill*, New York. See in particular expressions (1.22) and (6.22) corresponding respectively to LEE and simplified Lilley's equation.

References

[1]FREUND, J.B., 1999, Acoustic sources in a turbulent jet: a direct numerical simulation study, AIAA Paper 99-1858.

[2]COLONIUS, T., 1997, Lectures on Computational Aeroacoustics, *von Karman Institute for Fluid Dynamics*, Lectures Series 1997-07.

[3]BOGEY, C., 2000, *Calcul direct du bruit* aérodynamique et validation de modèles acoustiques hybrides, Ph. D. thesis of Ecole Centrale de Lyon, No. 2000-11.

[4]BOGEY, C., BAILLY, C. & JUVÉ, D., 2000, Computation of the sound radiated by a 3-D jet using Large Eddy Simulation, AIAA Paper 2000-2009.

[5]LIGHTHILL, M.J., 1952, On sound generated aerodynamically - I. General theory, *Proc. Roy. Soc. London*, **211**, A 1107, 564-587.

[6]RIBNER, H.S., 1996, Effects of jet flow on jet noise via an extension to the Lighthill model, *J. Fluid Mech.*, **321**, 1-24.

[7]LILLEY, G.M., 1972, The generation and radiation of supersonic jet noise. Vol. IV - Theory of turbulence generated jet noise, noise radiation from upstream sources, and combustion noise. Part II: Generation of sound in a mixing region, *U.S. Air Force Aero-Propulsion Lab.*, AFAPL-TR-72-53, Vol. 4.

[8]PRIDMORE-BROWN, D.C., 1958, Sound propagation in a fluid flowing through an attenuating duct, *J. Fluid Mech.*, **4**, 393-406.

[9]GOLDSTEIN, M.E., 1981, Aeroacoustics of turbulent shear flows, *Annu. Rev. Fluid Mech.*, **16**, 263-285.

[10]CANDEL, S.M., 1977, Numerical solution of conservation equations arising in linear wave theory: application to aeroacoustics, *J. Fluid Mech.*, **83**(3), 465-493.

[11]BERMAN, C. & RAMOS, J., 1989, Simultaneous computation of jet turbulence and noise, AIAA Paper 89-1091.

[12]BÉCHARA, W., BAILLY, C., LAFON, P. & CANDEL, S., 1994, Stochastic approach to noise modeling for free turbulent flows, *AIAA Journal*, **32**(3), 455-463.

[13]BAILLY, C., LAFON, P. & CANDEL, S., 1995, A stochastic approach to compute noise generation and radiation of free turbulent flows, AIAA Paper 95-092.

[14]LONGATTE, E., LAFON, P. & CANDEL, S., 1998, Computation of noise generation in internal flows, AIAA Paper 98-2332.

[15]BAILLY, C. & JUVÉ, D., 1999, A stochastic approach to compute subsonic noise using linearized Euler's equations, AIAA Paper 99-1872.

[16]TAM, C.K.W. & WEBB, J.C., 1993, Dispersion-relation-preserving finite difference schemes for computational acoustics, *J. Comput. Phys.*, **107**, 262-281.

[17]TAM, C.K.W. & DONG, Z., 1996, Radiation and outflow boundary conditions for direct computation of acoustic and flow disturbances in a nonuniform mean flow, *J. Comput. Acous.*, **4**(2), 175-201.

[18]BOGEY, C., BAILLY, C. & JUVÉ, D., 1999, Computation of mixing layer noise using Large Eddy Simulation, AIAA Paper 99-1871, accepted in the AIAA Journal.

[19]BAILLY, C. & JUVÉ, D., 2000, Numerical solution of acoustic propagation problems using linearized Euler's equations, *AIAA Journal*, **38**(1), 22-29.

[20]LEE, D.J. & KOO, S.O., 1995, Numerical study of sound generation due to a spinning vortex pair, *AIAA Journal*, **33**(1), 20-26.

[21]POWELL, A., 1964, Theory of vortex sound, *J. Acoust. Soc. Am.*, **36**(1), 177-195.

[22]COLONIUS, T., LELE, S.K. & MOIN, P., 1997, Sound generation in a mixing layer, *J. Fluid Mech.*, **330**, 375-409.

[23]MITCHELL, B.E., LELE, S.K. & MOIN, P., 1995, Direct computation of the sound from a compressible co-rotating vortex pair, *J. Fluid Mech.*, **285**, 181-202.

[24]GOLDSTEIN, M.E., 1976, Aeroacoustics, *McGraw-Hill*, New York. See in particular expressions (1.22) and (6.22) corresponding respectively to LEE and simplified Lilley's equation.